Title

Qualitative Analysis on the Performance of Non-uniform Platoons: Report I; Non-uniformities and Performance Issues

Authors

Tongue, Benson H.
Packard, Andy
Sachi, Paul

Publication Date

1997

CALIFORNIA PATH PROGRAM
INSTITUTE OF TRANSPORTATION STUDIES
UNIVERSITY OF CALIFORNIA. BERKELEY

Qualitative Analysis on the Performance of Non-uniform Platoons: Report I; Non-uniformities and Performance Issues

Benson H. Tongue, Andy Packard, Paul Sachi
University of California, Berkeley

California PATH Research Report
UCB-ITS-PRR-97-1

This work was performed as part of the California PATH Program of the University of California, in cooperation with the State of California Business, Transportation, and Housing Agency, Department of Transportation; and the United States Department of Transportation, Federal Highway Administration.

January 1997

ISSN 1055-1425

Qualitative Analysis on the Performance of Non-uniform Platoons: Report I, Non-uniformities and Performance Issues

Benson H. Tongue, Andy Packard, and Paul Sachi

Department of Mechanical Engineering
University of California at Berkeley

California PATH Program

Abstract

This is the first of two reports in which we detail the accomplishments and findings of a two-year research project aimed at determining control and spacing strategies as well as developing performance issues for automated vehicles traveling in platoons under non-uniform conditions. The first phase of the research was geared toward determining parameter uncertainty ranges for a given model and expected disturbances that materially affect the behavior of a vehicle in a platoon. Once this was completed, the relevant criteria for determining platoon performance were investigated. A simulation code was then written to evaluate platoon performance for a variety of platooning scenarios.

keywords: performance, platooning, safety, AHS

Nomenclature

A	vehicle frontal area (m^2)
a_b	braking deceleration (m/s^2)
a_h	tire hysteresis $(\mathrm{N/m})$
C_D	aerodynamic drag coefficient
$C_{D,un}$	percent uncertainty in aerodynamic drag coefficient
CR_a	correction factor for aerodynamic drag uncertainty bounds
CR_D	correction factor for aerodynamic drag drafting effects
CR_r	correction factor for rolling resistance uncertainty bounds
e_{ff}	drivetrain effectiveness, percent
e_{un}	percent uncertainty in engine effectiveness
F	total force acting on a car (N)
F_a	aerodynamic drag force (N)
F_b	brake force acting at the tire-road interface (N)
$F_{b,m}$	maximum brake force available at the tire-road interface (N)
F_e	engine force acting at the tire-road interface (N)
$F_{e,m}$	maximum engine force available at the tire-road interface (N)
F_g	gravitational force due to road grade (N)
F_r	rolling resistance force (N)
f_r	coefficient of rolling resistance
$f_{r,un}$	percent uncertainty in coefficient of rolling resistance
G_o	road roughness
GR	gear ratio reduction from engine shaft to wheel axle
g	gravitational acceleration $(\mathrm{m/s^2})$
h	axle height (tire radius, wheelbase) (m)
L_i	length of car i (m)
M	vehicle mass **(kg)**
M_{un}	percent uncertainty in vehicle mass
$PC(v)$	power curve function for engine torque $(\mathrm{N \cdot m})$
T_b	brake torque $(\mathrm{N \cdot m})$
$T_{b,m}$	maximum brake torque $(\mathrm{N \cdot m})$
T_e	engine torque $(\mathrm{N \cdot m})$
$T_{e,m}$	maximum engine torque $(\mathrm{N \cdot m})$
TR	road traction
v	velocity of vehicle $(\mathrm{m/s})$
v_w	velocity of wind $(\mathrm{m/s})$
α	brake input
Δ_i	space between front of car i and back of car $i-1$ (m)
$\Delta_{i,d}$	desired spacing between car i and car $i-1$ (m)

θ	road grade (rad)
μ	braking coefficient of friction
μ_{un}	percent uncertainty in braking coefficient of friction
ρ	density of air (kg/m^3)
τ_b	brake time lag (sec)
τ_e	engine time lag (sec)
ϕ	engine input
ω	engine speed (RPM)

EXECUTIVE SUMMARY

This report is part of an ongoing examination into the behavior of platoons under less-than-optimal conditions. One immediate source of non-optimality is the probable existance of quantitatively different vehicles making up platoons. Variations in engine effectiveness, braking effectiveness, mass, planform, etc. all combine to make the control task more difficult. Besides non-uniformity among vehicles, non-nominal operating conditions such as emergency maneuvers, vehicle entry/exit, sensor noise, road surface condition, wind gusts, and road grade will also tend to degrade platoon performance.

An attempt is made herein to quantify the parametric uncertainties for a wide range of vehicles. Several nominal vehicle models have been previously developed, yet the available data for expected ranges of parametric variations of more complex models is quite limited. A simplified model has been chosen in which parameter variations can be most easily quantified while still retaining modeling fidelity.

This information provides the groundwork for further research into platoon optimization. The end-product will be computational code that will determine how "good" a given platoon is and will thus permit an evaluation between competing platoon designs. The quality of the platoon will be measured with respect to a user definable performance index, thus allowing the designer to optimize the platoon structure for the particular operating conditions of interest.

Contents

1 INTRODUCTION

Over the past several decades, the number of vehicles on roads has been steadily increasing. In order to alleviate the attendant overcrowding, several strategies to increase throughput are being developed. One suggestion, part of the IVHS (Intelligent Vehicle Highway Systems) effort, has been for automobiles to travel in platoons guided by on-board computers. Platoons are composed of several closely-spaced vehicles traveling on a highway lane that has been specially designated for platoon activity. When a vehicle enters a platoon lane, control of the car is switched from the driver to the car's on-board computer. Equipping vehicles with platooning capabilities would theoretically increase throughput on highways since increased tracking accuracy and reduced reaction time over that of human drivers could permit much smaller vehicle to vehicle spacings than is possible for vehicles under human control. Along with this increase in performance, however, must come a high level of safety. Control strategies must therefore be developed and tested for all circumstances that could possibly arise during platooning operations.

Previous work in designing controllers and simulating platoon behavior has invariably assumed that car to car vehicle characteristics are uniform within a platoon. However given the current influence of consumer preferences in automobiles, it is probable that many vehicles, having various styles, makes, acceleration capabilities, etc. will ultimately be employed. In addition, aging, wear, loading, and other factors which will induce parametric uncertainty will contribute to platoon non-uniformity. Research by Tongue and Yang [33] has indicated that platoon performance deteriorates when controllers designed for uniform vehicles are employed in vehicles with small parameter variances, thus motivating a concern into the broader question of platoon behavior in the face of uncertain platoon parameters.

Besides non-uniformity among vehicles, non-nominal operating conditions such as emergency maneuvers [34], vehicle entry/exit, sensor noise, road surface condition, wind gusts, and road grade will also degrade platoon performance. Figure 1 shows the effect of road grade on spacing response with all other conditions nominal when a platoon travels over a triangular hill of grade $\approx 1\%$. Here, this relatively small disturbance produces a 4% error in the spacing response. Combining disturbances with parametric uncertainties could produce severely degraded operations. Thus a need exists to design controllers and develop spacing algorithms to account for non-uniformities.

An attempt is made herein to quantify the parametric uncertainties for a wide range of vehicles. Several nominal vehicle models have been previously developed [2, 15, 21, 26, 29, 32], yet the available data for expected ranges of parametric variations of more complex models is quite limited. A simplified model [32] has been chosen in which parameter variations can be most easily quantified while still retaining modeling fidelity.

Once parametric uncertainties and exogenous inputs are determined, a criteria for evaluating performance will need to be developed. Then, by altering parameters and input signals through numerous simulations, the worst expected platoon operating conditions for

a given controller and spacing strategy can be found and compared to acceptable performance ranges. This effort requires that the simulation code be modular for ease in switching controllers and other components. We will also propose a standard for vehicle modeling to allow for components from other research areas to be implemented.

2 MODELING

The platoon and vehicle model considered for this research is similar to that developed by Sheikholeslam and Desoer [21]. The platoon contains closely-spaced, longitudinally aligned vehicles traveling along a highway, with the acceleration/deceleration of each vehicle controlled by on-board computers. Controller inputs are retrieved from sensors and from information transmitted between vehicles and the platoon system hierarchy. This study's model diverges from that of [21] in the number and complexity of the forces acting on the vehicles.

2.1 Platoon Model

Figure 2 shows a platoon of three vehicles and a lead car with the origin of the Cartesian coordinate frame associated with each vehicle located at the vehicle's rear. Each vehicle is of length L; and is spaced **A;** meters behind the preceding vehicle. The lead car, a fictitious vehicle, is assumed to follow desired acceleration (or velocity) trajectories perfectly while each of the following vehicles attempts to maintain a desired spacing of $\Delta_{i,d}$ meters between itself and the preceding vehicle.

2.2 Vehicle Model

A simple vehicle model is shown in Figure **3.** The external forces (aerodynamic drag, rolling resistance, and gravitational force) are summed with the forces acting at the tire-road interface produced by the braking and powertrain systems. The controller supplies the inputs to the engine (throttle angle ϕ) and brakes (brake actuation α).

Extensive research in modeling each of these components has already been undertaken [2, 13, 15, 16, 21, 22, **30,** 32, 34]. The object of this report is not to develop new modeling but to quantify and bound the parameter variances that might occur in models previously developed. The following is a description of model components for which parameters and their associated uncertainties were obtained for a variety of vehicles.

2.2.1 Powertrain model

The powertrain in this report includes an engine, transmission, and drivetrain (carried to the tire-road interface). **A** nine-state powertrain model was developed by Cho and Hedrick [2] using physical principles, and Tongue and Yang [32] have developed a reduced-order model (ROM) of the nine-state model to decrease simulation time. The ROM (see Equations 1–3) is essentially a saturation limit to the powertrain output followed by a first-order time lag. The details of these two models, their state equations, derivations, and simulation results can be found in each of the above references.

The nine-state and ROM models require knowledge of several parameters for a given drivetrain. Parametric uncertainties due to wear, age, and other factors for a wide range of drivetrains is not readily available. If the saturation limit in the ROM is replaced with a saturation limit based on engine power curves, $PC(v)$, then the task of determining the uncertainties for numerous parameters is reduced to determining the uncertainties in the engine power curve and the drivetrain efficiency. These will be lumped into one uncertainty for engine effectiveness, e_{un}.

Engine power curves provide a relationship between engine speed and maximum power output or maximum torque of an engine. If we assume the engine shaft, gears, axles are approximately rigid and the axle height is constant, the engine speed equals the car velocity times the gear ratio divided by the axle height ($\omega = v \cdot GR/h$). The power curve can then be expressed as a relation between velocity and maximum torque. The engine force at the tire-road interface is determined by transmitting the torque delivered by the engine through the drivetrain and multiplying by a factor for efficiency e_{ff}. The maximum engine force acting at the tire-road interface, $F_{e,m}$, is then a function of $PC(v)$, e_{ff}, GR, and h (see Equation 4).

The gear ratios will change as a function of engine speed. For each gear, when the engine speed reaches the maximum RPM for that gear, the transmission will shift up to the next gear and GR will change. The transmission down-shifts and GR changes when the engine speed is at the minimum for that gear. The engine speed is not allowed to fall below the minimum engine speed in 1st gear or go above the maximum engine speed for the highest gear. Currently, no dynamics are incorporated with the transmission; the gear shifting is assumed to be instantaneous. Appendix **D.4.1** provides an example of the gear shifting mechanism.

Power curves for 4, 6 and 8-cylinder engines were obtained from car manufacturers. Figure 4 compares the open throttle response of a BMW M3 [1] with a computer simulation using the ROM with the saturation limit replaced by $PC(v)$ and assuming $e_{ff} = 80\%$. As can be seen, the velocity difference between the two results is no greater than ± 1 m/s at any instant in time. Also, the acceleration between 20 and 30 m/s, the range of velocities for most platoon operations, are nearly identical.

2.2.2 Brake model

The brake system is composed of air brake lines, regulators, actuators, and brake drums or discs operating on the wheel. The torque delivered to the tires is modeled by McMahon and Hedrick [15] as a first-order lag (Equation 6).

We assume that all cars will be operating with an anti-lock brake system (ABS). When the brake torque is high, the ABS will attempt to operate around the peak coefficient of tire traction, The ABS performance will be defined as the average braking coefficient μ, the ratio of brake force to normal force when the road traction is 1. Assuming the axle height is

constant, the maximum torque delivered by the brakes is then a function of μ, road traction (see Section 3.2.4), vehicle weight, and axle height (Equation 7).

2.2.3 Aerodynamic drag

Most models of aerodynamic drag forces contain a relationship involving the aerodynamic drag coefficient, frontal car area, air density, and relative air speed [2, 15, 21, 29]. We will include a correction factor for the aerodynamic drag coefficient (Equation 9) as suggested by Tongue et al. [30] since aerodynamic forces are reduced when vehicles are spaced closely together. The non-uniformities we will consider for this model are the aerodynamic drag coefficient and wind speed.

2.2.4 Rolling resistance

Rolling resistance is a complicated force to determine. The coefficient of rolling resistance, f_r, depends on engine speed, vehicle velocity, road roughness, tire properties, etc. Tongue et al. have developed a simplified model [32] of f_r, based on research by Lu [13], where f_r is a function of vehicle velocity and road roughness, G_o (Equations 12– 11). In deriving the original relationship, Lu showed f_r depends also on tire hysteresis, a_h, and axle height, h; we include these parameters in determining the coefficient of rolling resistance (Equation 13). Non-uniformities due to uncertainty in f_r $(f_{r,un})$, vehicle mass, (M_{un}) and variances in road grade (6) will be considered here.

2.2.5 Gravitational force

The simple physical relationship used in modeling the gravitational force due to road grade [2, 21, 32] is given in Equation 14. The important variances to consider here are M_{un} and 6.

2.3 Controller Model

In consonance with previous PATH research, this report assumes that each vehicle is equipped with sensors to measure its own velocity and acceleration as well as the space between the preceding vehicle and itself. Intra-platoon communication will transmit sensor readings for the preceding vehicle's velocity and acceleration as well as the lead car's velocity and acceleration. These sensor readings will constitute the controller inputs. The current communications delay and update rate for the sensors are both 0.02 sec; these delays are included in the model.

The controller currently employed was originally designed by Sheikholeslam and Desoer [21, 22, 23, 24, 25]. The control approach linearizes the vehicle model and controls the third derivative of the vehicle's position. Although the vehicle model has been updated, research by Tongue et al. [32, 33, 34] has shown that the controller still performs well.

Other controllers have been designed for a variety of inputs and vehicle models (see especially Swaroop's paper [29]). Since the performance of each controller depends on the model considered, an evaluation of every controller will not be made here. However, the simulation code is designed to allow for the interchanging of controllers and vehicle model components (see Section 5.1).

3 NON-UNIFORMITIES

Non-uniformities include parameter uncertainties, exogenous inputs, and noise. The parametric uncertainties considered will materially affect the performance of a nominally uniform platoon operating in a known environment; a robust control strategy must be designed to minimize their influence.

3.1 Parametric Variations

The assumption that all vehicles within a platoon are identical is an attractive one for analysis but unlikely in reality. The historical trend to meet consumer preferences has always resulted in a wide variety of cars of differing makes, models, types, costs, etc. We will assume in the following that every vehicle can be modeled as previously presented by appropriately changing car parameters and engine power curves. However, parameters for a given vehicle will change due to loading, wear, age, and other factors, giving rise to parametric uncertainty. For this study, the nominal parameters are calculated to be the average of the maximum and minimum parameters, and a parameter variance is then applied.

3.1.1 Engine effectiveness

The main variances to be considered in the engine model of Section 2.2.1 are changes in the power curve and drivetrain efficiency. Since both of these terms affect the engine force transmitted to the tires, we will consider a parameter which accounts for variations in the engine force, or, engine effectiveness, carried through the drivetrain, e_{un}. These deviations arise from measurement inaccuracies, engine wear, aging, dirt, corrosion, etc. Long-term performance tests have been conducted on a wide range of vehicles [1]. For the cars considered, the average change in acceleration for a 0 to 60 MPH start ranged from -6.25% to +11.77%, with an absolute average value of 2.86% (more accelerations decreased over time than increased). Incorporating error in the test procedure, the small number of vehicles tested, and the limited scope of acceleration tests, we will assume that the e_{un} is bounded by $\pm 15\%$ for all engine operating conditions.

3.1.2 Braking coefficient of friction

The factors which will change the braking coefficient μ by more than $\pm 2\%$ for a given vehicle and tire are tire pressure (wet surfaces), ambient temperature (wet surfaces), initial speed when braking (wet surfaces), treadwear (wet surfaces), repeatability, and loading. Tire pressure has only a negligible effect on vehicle operation for dry surfaces, but has been shown to produce up to a $\pm 0.1\%$ change in μ per $\mathrm{kN/m^2}$ [6] (roughly $\pm 3.5\%$ for an expected f 5 psi change) when operated on wet surfaces. The ambient temperature could affect μ by up to

$\pm 8\%$ [5] for wet surfaces. For dry roads, the initial braking speed has little effect on μ, but could decrease the coefficientof friction by .025 per velocity increase of 1 m/s for wet roads; this results from decreased amount of time for water to escape the contact area between the tire and road [3, 6, 7]. Treadwear increases μ only slightly for dry roads, but could drop the friction coefficientby 10% for heavily worn tires and up to 40% for bald tires on wet surfaces [6, 8]. Repeatability of brake tests were found to be within $\pm 7\%$ [3, 7, 14]. Increasing the vehicle load by 100 kg decreased μ up to .02 on dry surfaces and .009 on wet surfaces [3].

Since the relationship between the above variances is not known, and because the effects of some factors are linear and others are a percentage change, the determination of μ_{un} will be estimated. Hiltner et al. [7] have conducted testing on light vehicle **ABS** performance. In their report, stopping distances are measured for different vehicles, loadings, test surfaces, and initial speeds. Assuming the braking deceleration a_b is constant, a_b equals the initial velocity squared divided by twice the stopping distance. Since μ is defined **as** the ratio **of** the braking force to normal force, $\mu = M \cdot a_b / M \cdot g = a_b / g$. From the data presented in that report, the maximum variance in μ for a given passenger vehicle and road surface was found to be $\pm 16.3\%$ (Chrysler Imperial on wet polished concrete); this takes into account the combined effects of loading, initial speed, and repeatability. Considering the other factors which would vary μ **as** mentioned above, we will assume the bound for μ_{un} is $\pm 25\%$ for the work to follow.

3.1.3 Mass

Vehicle mass will vary with loading. Ideally, a sensor would be used to measure the mass **of** the loaded vehicle before it entered the platoon lane. In this case, the mass would change by the amount of fuel that is consumed while the vehicle is in motion, a variation that is easily accounted for. For this study, however, we will assume that no such sensor is employed.

The vehicle weight will be allowed to vary from curb weight to gvwr (gross vehicle weight rating) **as** specified by the manufacturers. The nominal mass will then be the median of these two masses, and the range of uncertainty for the mass, M_{un}, will be easily determined. For most small to mid-sized passenger vehicles, the expected bound for M_{un} is $\pm 12\%$.

3.1.4 Aerodynamic drag coefficient

In general the aerodynamic drag coefficient depends on the exterior vehicle dimensions and is attainable from car manufacturers. Luggage racks, bikes, and other objects mounted to a vehicle will change this coefficient by an appreciable amount. Currently, we do not have data available on the range of deviations that might occur. Therefore, we estimate the area of a large item mounted to a vehicle to be 0.60 m^2, about a 35% increase for small cars. Normalizing the relationship for aerodynamic drag (10) produces a range of $\pm 15\%$ for the uncertainty in aerodynamic drag coefficient, $C_{D,un}$.

3.1.5 Rolling resistance coefficient

The effect of road roughness G_o on the rolling resistance coefficient f_r for most highways will change by $\pm 5\%$ (**12).** Since this effect is not large, it will be captured in the uncertainty factor for f_r ($f_{r,un}$) instead of adding an exogenous input for road roughness. The coefficient of rolling resistance has been shown [19] to depend mostly on road roughness, tire pressure, tire temperature, and vehicle velocity.

For a ± 33 kN/m^2 change in tire pressure, f_r changes by $\mp 2.5\%$. Temperature of the tire, which effects the properties of tire hysteresis ***(ah),*** varies f_r by $\pm 5.4\%$ per $\mp 10^o$ C after the tire has been in operation for ten minutes. We will assume the vehicle has been operating for at least ten minutes for the temperature of the tire to be fairly constant and change by only $\pm 10^o$ **C.** Vehicle speed can influence tire hysteresis by increasing a_h up to **10%.** Tire slip angle will not be considered in this analysis since this model is only concerned with longitudinal motion, although a slip angle of 2% has been shown [19] to have a large effect on f_r.

Additively combining these effects produces an error in f_r of -8% to $+28\%$ for most steady-state vehicle operating conditions. Equation **12** is rewritten to include the parameters mentioned above and is averaged between the maximum and minimum values of f_r resulting in $f_{r,un}$ being bounded by $\pm 16\%$ (**13).**

3.2 Exogenous Inputs

Exogenous inputs encompass disturbances and noise. These will be considered as signals external to the platoon that can vary with time, whether the source is lead vehicle commands from the control center, road profiles, weather conditions, or sensor noise. Our desire is to determine input bounds for various platooning scenarios. Additionally, we will consider filtering the frequency content of the inputs since the worst case performance algorithm presented in [31] may produce random signals which would not correspond to expected inputs. The considerations for filtering will be discussed here, and the filters used for the algorithm will be addressed in [31].

3.2.1 Lead car acceleration profile

We assume that the lead car will receive acceleration commands (or velocity if needed) from the control hierarchy. Throughout most platoon operation, the vehicles should be traveling at constant speed. When exit/entry maneuvers or an emergency situations occur, however, the platoon will need to accelerate and/or decelerate.

The magnitude of accelerations we expect for nominal operation will be at most $0.1g$. For strong acceleration/deceleration, we would expect up to $0.2g$. For emergency cases, we will consider that the lead car might receive a deceleration command for a dead stop, or an acceleration command as high as the maximum acceleration attainable by the vehicles in the platoon.

We will assume that most commands from the control center will have low frequency content since most signals should be relatively smooth. Sine acceleration profiles, or $1-\cos$ curves for velocity profiles, will be used to model the control commands. Also, the commands for entry/exit maneuvers are expected to occur at most about once every ten seconds.

3.2.2 Wind

When vehicles are traveling at high speeds, the force due to aerodynamic drag can be quite large. Since aerodynamic drag depends on the square of relative air speed, wind can greatly influence the tracking performance of vehicles in a platoon. We will consider the maximum limits on wind gust speed to be $f20$ m/s, and the variations of wind speed for a given scenario to be ± 10 m/s. The wind gusts are considered to be random sinusoidal signals with frequency generally less than 0.2 Hz. This will be modeled as a random signal filtered with a linear first-order low-pass filter with a break frequency at 1.256 rad/s.

3.2.3 Road grade

Road grade obviously effects the gravitational force acting on a vehicle. According to the US Department of Transportation, the grade for freeways should not exceed 6% (mountainous

terrain). A range of $\pm 3\%$ will be used in this study. **Also,** we will assume the frequency of traveling over a hill is not much greater than 0.05 **Hz** (about one hill every 500m).

3.2.4 Road traction

When braking, the maximum deceleration of a vehicle depends primarily upon the amount of friction at the tire-road interface. Road texture, material composition, and weather conditions all significantly impact road traction **[3,** 6, 7, 20].

Water on the road is the largest contributor to the decrease in available traction. On average, the coefficient of friction decreases by **30%** for a 0.05 cm rainfall [3]. More water increases the chance of hydroplaning; a drop in the coefficient of friction by about 0.10 is expected. We will not consider flooding or roads covered with snow and ice. The pavement microtexture and macrotexture alter the coefficient of friction for dry roads by $\pm 5\%$ and by $\pm 25\%$ for wet roads **[6]** (texture effects the rate of water drainage). Additionally, road roughness has been shown to decrease the coefficient of friction by 0.04 for an increase in the road roughness power spectral density from 0 to 11 **Hz.**

In a report by Ebert [3], several tests were performed to determine the peak coefficient of friction while braking in various road conditions (as mentioned above), with different vehicle loadings, and using different initial speeds. To find the maximum road traction, we averaged the maximum peak coefficients recorded for the different loadings and initial speeds; this was done instead of choosing the overall maximum to eliminate the effects loading and speed have on the peak coefficient which were accounted for in μ_{un} **as** discussed in Section **3.1.2.** The same method was used to determine the minimum road traction. The resulting range of road traction was found to be 0.52–1.01.

Overall, road traction should not vary much with time. One case in which the traction can vary rapidly occurs when a platoon travels over a road with several puddles and dry patches resulting from a rainstorm followed by a sunny day. We will assume that the time for entering one puddle to the next while traveling on a highway is usually not more than 10 seconds, or about one cycle per 250m. For a random signal, a first-order low-pass filter with a pole at -0.628 rad/s will be used.

3.2.5 Sensor noise

Most data available for sensor noise indicates that the sensor signal is usually clear but that the sensors often fail in obtaining a reading and return a zero or other default value. We will assume that if a sensor fails to obtain a reading, the previous reading will be returned instead of the default. The sensor noise we will consider is a white noise signal with frequencies generally greater than 50 Hz and with a sensor signal to noise ratio of 20.

4 PERFORMANCE EVALUATION CRITERIA

In this section we discuss the criteria we consider relevant in determining a performance index through which platoon simulations can be evaluated.

4.1 Vehicle Ride Quality

Research has indicated that vehicle passenger ride quality is closely related with acceleration frequency content [4, 10, 12, 28]. Previously, Tongue and Yang [35] considered evaluating ride quality using a Mean Personal Rating (MPR) measure. This measure was based on a method by Smith et al. [28] for determining ride comfort using vertical acceleration profiles. The frequency content of the longitudinal acceleration profiles for vehicles in a platoon were weighted according to the scaling for vertical accelerations. Since human whole-body vibrations are different in these two directions, an alternative weighting is considered in this report.

Leatherwood and Barker [11] present a computer tool to estimate the ride quality of helicopters and automobiles for combined motion in six directions. To obtain an estimation of the ride quality as presented in [11], the power spectral density of translational acceleration along each coordinate axis and angular acceleration about each axis must be computed. The power spectral densities are then weighted. The weighting functions were obtained experimentally by subjecting a population to a series of vibration tests at different frequencies and magnitudes. The weighted power spectral density is used to determined the weighted root mean square acceleration for each profile. The root mean squares are then combined to determine the discomfort number, DISC. The DISC is related to a function which predicts the fraction of the population that would regard the ride as uncomfortable.

In our use of the comfort index, the algorithm by Leatherwood and Barker is employed for longitudinal acceleration only (Appendix C). The weighting function for the acceleration power spectral density in this direction is shown in Figure 5; the range of weightings is 0.5–12 Hz. Frequencies above 10 Hz are generally not noticed by passengers. On the other hand, frequencies below 1 Hz may cause motion sickness in some passengers; this effect depends on complicated factors varying among individuals and has not been found to relate to the frequency content of an acceleration signal [4]. (This effect will be neglected in performance calculations.)

4.2 Other Criteria

In addition to rider comfort, several other factors are considered in evaluating a platoon. These include:

- maximum spacing error

- average spacing error
- maximum acceleration levels
- number of collisions
- severity of collisions - total power absorbed
- fuel usage
- control activity / actuator use
- highway throughput / platoon length

With respect to the number of collisions, one point to consider is whether the collisions occur at the same instance or whether they occur at different times. Distinguishing between these two cases is relevant **if,** for example, all four cars in a four-car platoon collide because of *a* difficult maneuver (resulting in four collisions) versus one car colliding with another vehicle four times where one collision results from a difficult maneuver, and the other three occur during nominal operation. Obviously, the collisions occurring during nominal operation should be more heavily weighted.

5 SIMULATIONS

Now that a platoon model has been established and the background needed for calculating performance has been presented, the software and code used to perform platoon simulations will be presented. Also included is a data base of a possible input profiles which encompass most types of platooning scenarios we would expect. We have begun simulating various platooning scenarios and collecting data for evaluating platoon performance.

5.1 Simulation Code

The simulation code was originally written by Yang [35] using Simulink (Dynamic System Simulation Software by MathWorks Inc.) and Matlab M-files. This code has been rewritten for the model presented (Section 2) and extended to incorporate platoon non-uniformities (Section 3).

Figure 6 shows a Simulink model of a car. Each model component labeled in capital letters represents a Mex-file (C-coded M-file) S-function. Mex-files, in general, greatly reduce simulation time over M-files. S-functions allow the user to easily code any dynamics of the form $\dot{x} = f(x, u, t)$, $y = g(x, u, t)$. (See *Sirnulink User's Guide* [27] for more information on S-functions.)

The current simulation code has the advantages over Yang's code of reducing simulation time by a factor of five, having modeling components easily interchanged – modularity, and allowing the parameters as well as uncertainties to be changed from the Matlab workspace. The following standard is assumed for each modeling component:

- SENSORS: Inputs are car ID number, position, velocity, and acceleration (these four will be referred to as "states" though they are not the actual states of a car) for the previous car, following car, lead car, and the car itself. In the current sensor model, the outputs are sensor readings of spacing ahead, velocity, and acceleration of the car as well as communication of velocity and acceleration for the previous car and lead car.
- CONTROLLER: Inputs are sensor outputs; outputs are control commands to the engine and brakes.
- EXOGENOUS FORCES: Inputs are wind velocity, road grade, and "states" for the car itself, the previous car, and the following car. (The previous and following "states" are employed for determining the aerodynamics drag when drafting.) The output is the sum of exogenous forces acting on the car.
- BRAKE DYNAMICS: Inputs are road traction, control commands, and car "states"; output is the brake force acting at the tire-road interface.
- ENGINE DYNAMICS: Inputs are road traction, control commands, and car "states"; output is the engine force acting at the tire-road interface.

- PLANT: Inputs are the forces from Exogenous Forces, Brake Dynamics, and Engine Dynamics S-functions. The outputs are the "states."

5.2 Data Base

A data base has been created containing the input profiles for lead car acceleration, wind gusts, road grade, and road traction which we will consider for simulations. Appendix B contains a list of the current profiles. Although this list is not exhaustive, it does contain the list of inputs we would expect during platoon operation while covering the extremes. As research continues and more data is available for the types of inputs to expect, the list should be extended.

5.3 Simulation Results

Noteworthy results obtained from performing various simulations using the software code and the input profiles in the data base are presented and commented on in this section.

5.3.1 Exogenous inputs

The controller has no knowledge of the exogenous inputs. Figure 1 shows the spacing response of a 2-car platoon operating under nominal conditions while traveling over a triangular hill with the road grade slightly less then 1%. While the vehicles are subject to this road grade disturbance, the steady-state spacing error is about 0.04 m. To avoid large steady-state errors from greater disturbances, an integral term should be added to the existing controller to eliminate steady-state errors, or the controller should be redesigned to account for disturbance inputs.

We added an integral term for the spacing error with a gain of 80 in the controller. Figure 7 shows the spacing response of a platoon subject to the same inputs. The spacing response shows the spacing error begins to increase once a change in road grade is encountered but decreases and shows little to no spacing error after a few seconds. Also, the maximum magnitude of error is about one-fifth of the error when a controller with no integral term was employed.

5.3.2 Parametric variances

Figure 8 contains the spacing errors of 4-car platoons following the "smooth" lead car acceleration profile in Appendix B.1. In the first plot, the vehicles are identical and no disturbances are introduced; each spacing error response is approximately the same. The second plot shows the error response for a mass uncertainty of 10% in car 2 and -10% in car 3. Here, the magnitude of the error increased by about 20% for the second car and decreased

by nearly 20% for the third. We can conclude that parametric variances significantly impact the vehicles' spacing responses.

Ideally, we would be able to determine the error response sensitivity for each parametric uncertainty independently. The worst case performance could be found by combining the worst responses for each individual parameter. However, due to the nonlinear nature of the system, the sensitivity is dependent on the inputs and the other parameters.

5.3.3 Non-identical vehicles

For these simulations, we want to gain insight into the effect different cars would have on an error response. The first plot in Figure 9 shows the spacing error for a 3-car platoon of identical vehicles, BMW M3s, with the "sudden" lead car acceleration profile (Appendix B.1). The second simulation employed three different cars: a BMW M3, a Chevrolet Cavalier, and a Monte Carlo 234. For the most part, the error responses between the simulation with identical vehicles and different vehicles are the same. But, while the vehicles are accelerating, the Monte Carlo is approaching its acceleration limit and its spacing error begins to significantly increase.

The controllers, which are dependent on the car parameters, seem to perform similarly regardless of the vehicle as long as the desired control force is within the vehicle's operating range, *i. e.* regardless of mass, aerodynamic drag, etc., there is no apparent effect unless available engine power or braking force is insufficient. When encountering platooning scenarios which may encroach vehicle limitations, control strategies should be considered to avoid problems that would arise, especially in emergency situations which would undoubtedly test vehicle limitations.

5.3.4 Vehicle ride quality

Figures 10 a) and b) show the lead car velocity and acceleration profiles, respectively, for an "emergency" platooning scenario (Appendix B.1). The vehicle ride quality DISC number, as described in Section 4.1, for this profile was calculated to be 0.1293, a ride environment that would be considered comfortable by most passengers. The velocity response of a platoon attempting to follow this profile is shown in Figure 10 c). The DISC numbers for the four cars were 9.1889, 8.2181, 7.5535, and 5.4102, respectively; a DISC number above 3 is considered uncomfortable by most people. For emergency situations the current controller and spacing strategy produce extremely unpleasant ride environments although the lead vehicle ride quality is within acceptable ranges. When the platoon is simulated using less severe lead car acceleration profiles (*i. e.* "sudden" and "smooth" profiles in Appendix B.1), however, the DISC numbers for the vehicle responses are much closer to the lead car profile's DISC number. Therefore, a need exists to redesign the controller and spacing control strategy so that the platoon would react differently to improve platoon performance in emergency

situations.

a)

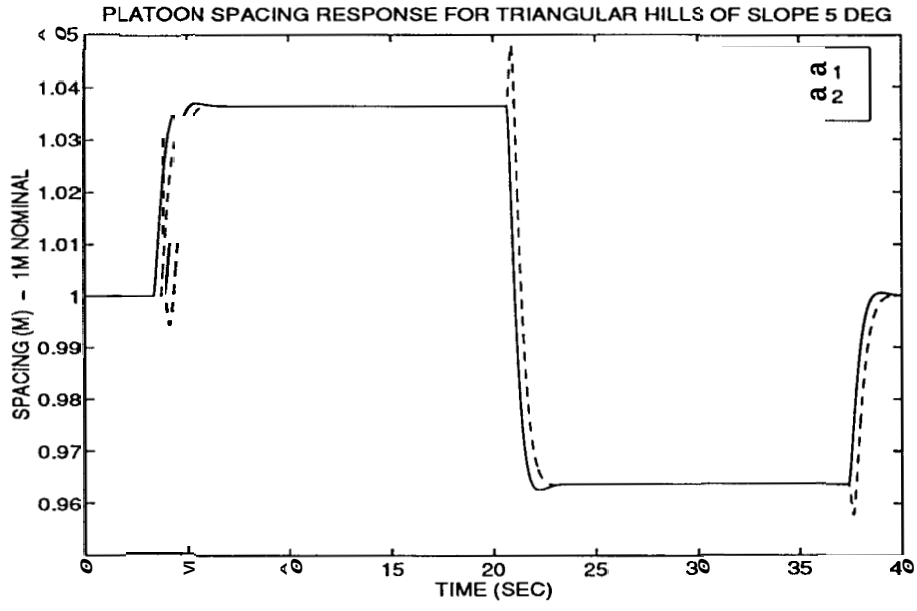

b)

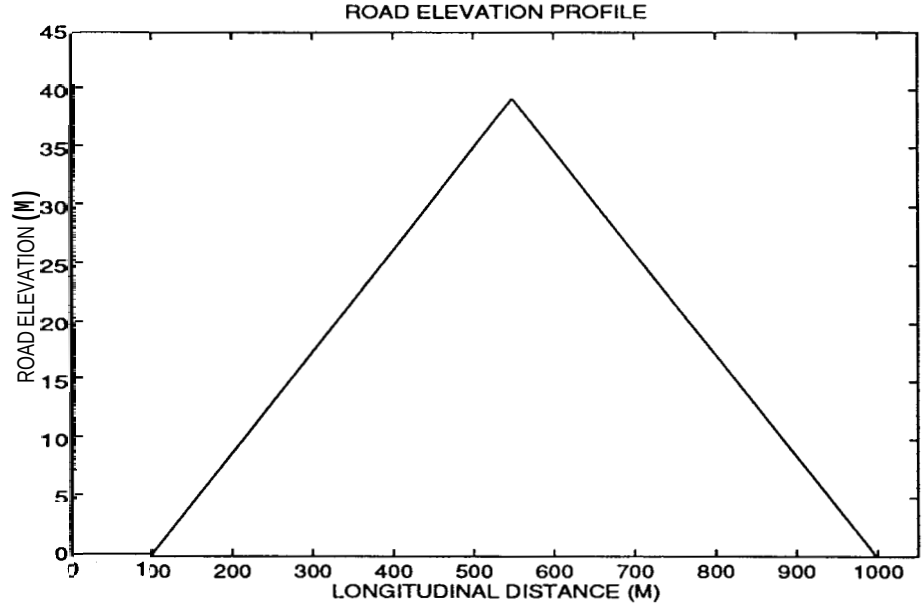

Figure 1: Spacing Response of a Platoon and Road Elevation Profile for a Platoon Simulation

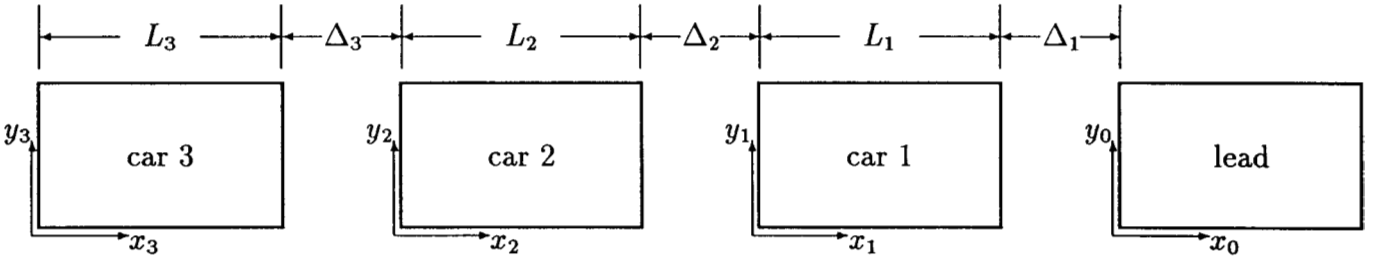

Figure 2: Model of a 3-car Platoon with Lead Car

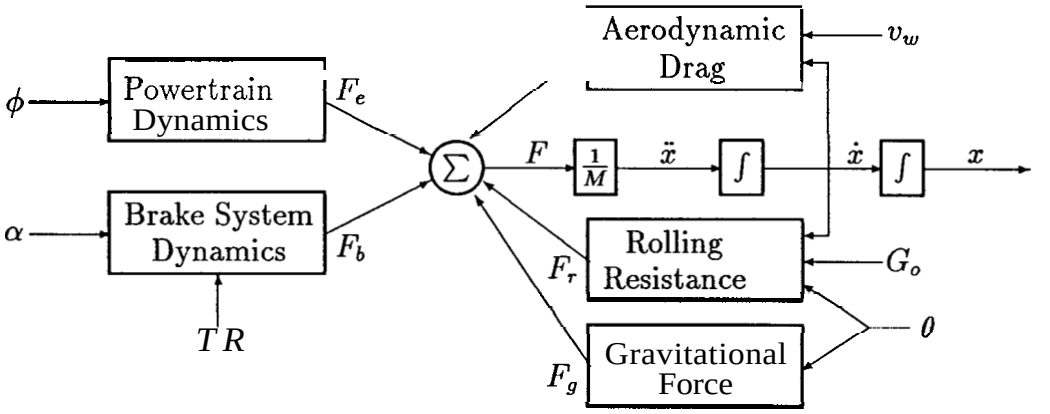

Figure 3: Simple Model of a Vehicle

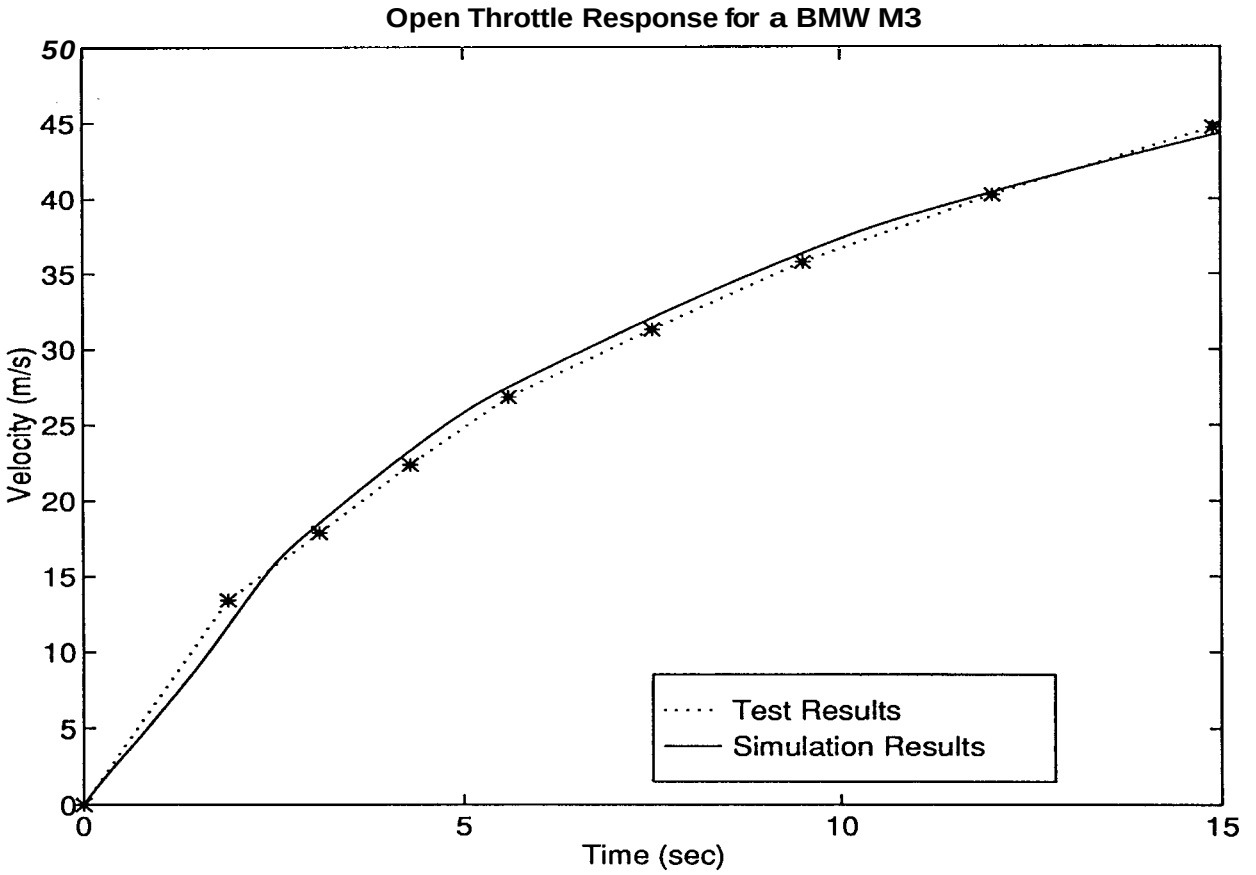

Figure **4:** Test and Simulation Results for the Open Throttle Responses of a BMW **M3**

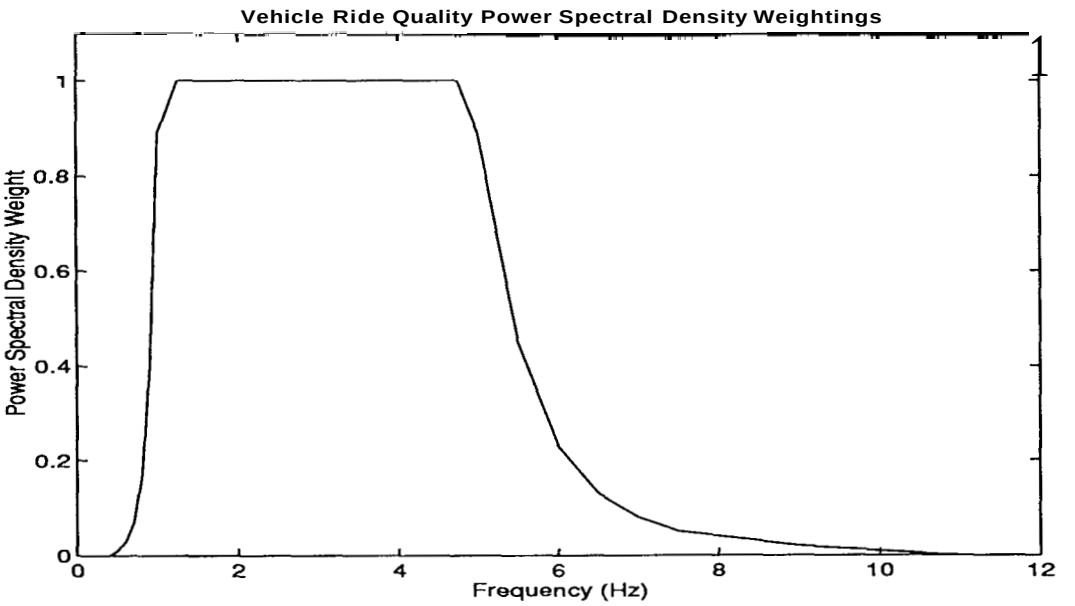

Figure 5: Longitudinal Acceleration Power Spectral Density Weightings for Vehicle Ride Quality Calculation

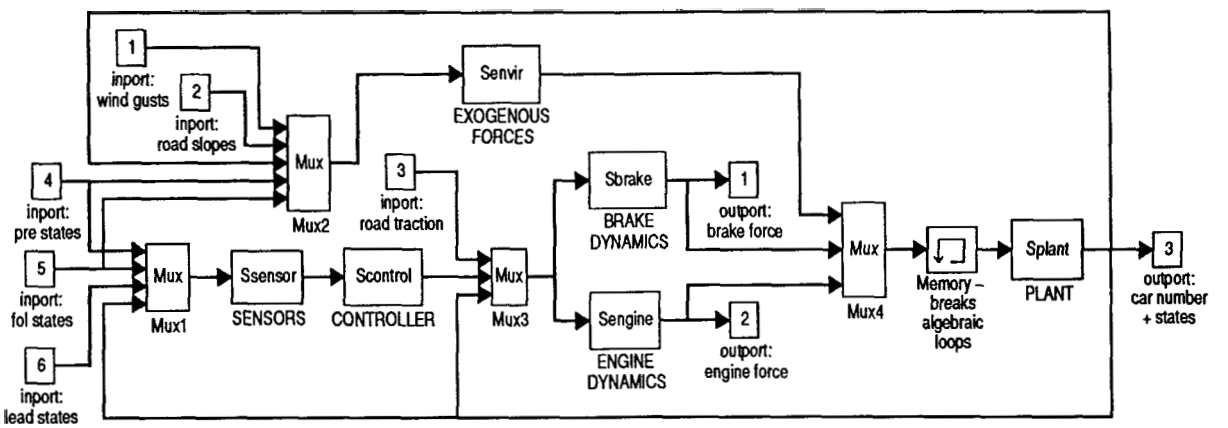

Figure **6:** Simulink Diagram of a Car Model

a)

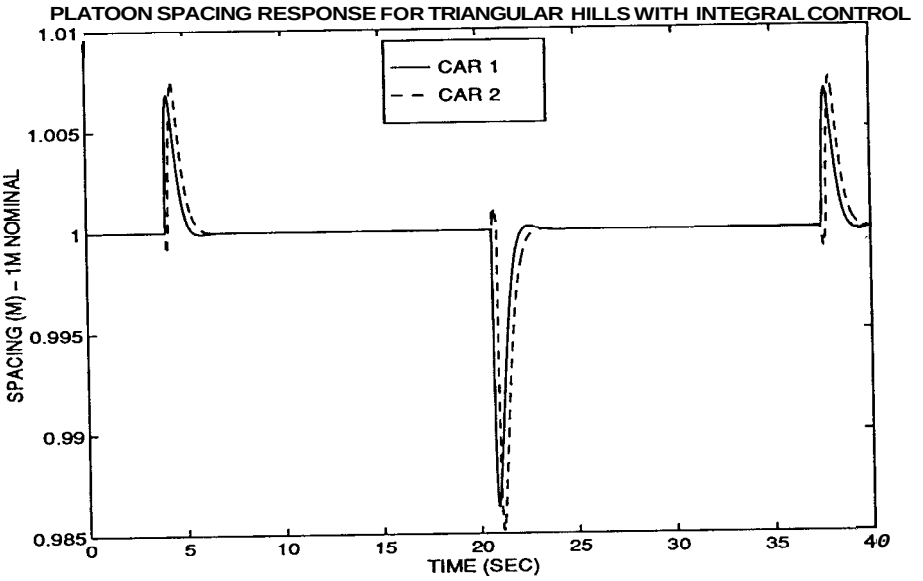

b)

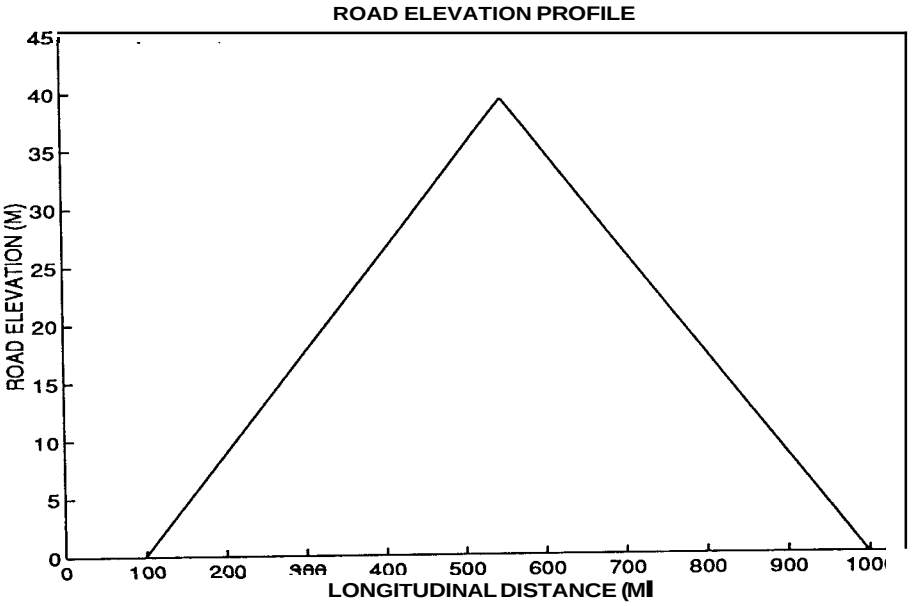

Figure 7: Spacing Response of a Platoon with an Integral Spacing Error Term in the Controller and Road Elevation Profile

a)

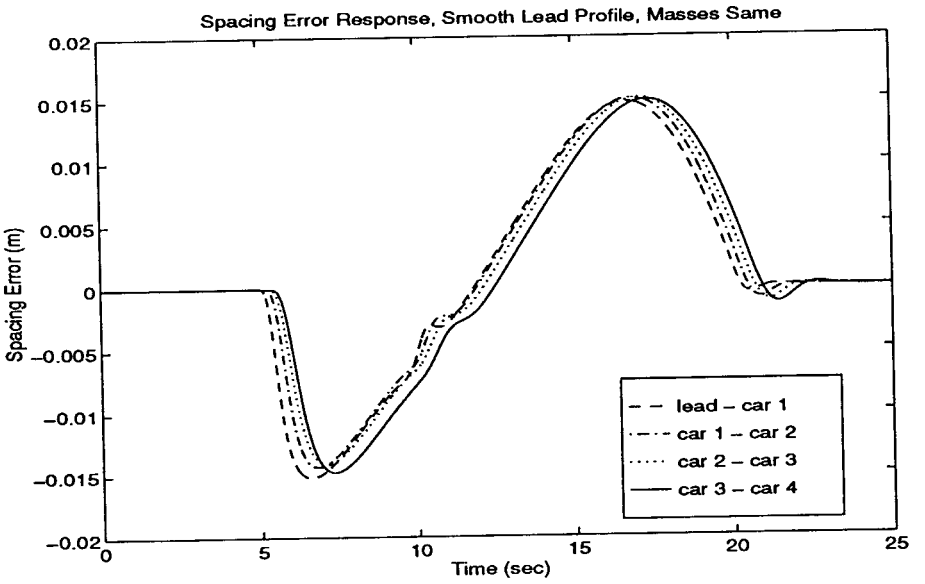

b)

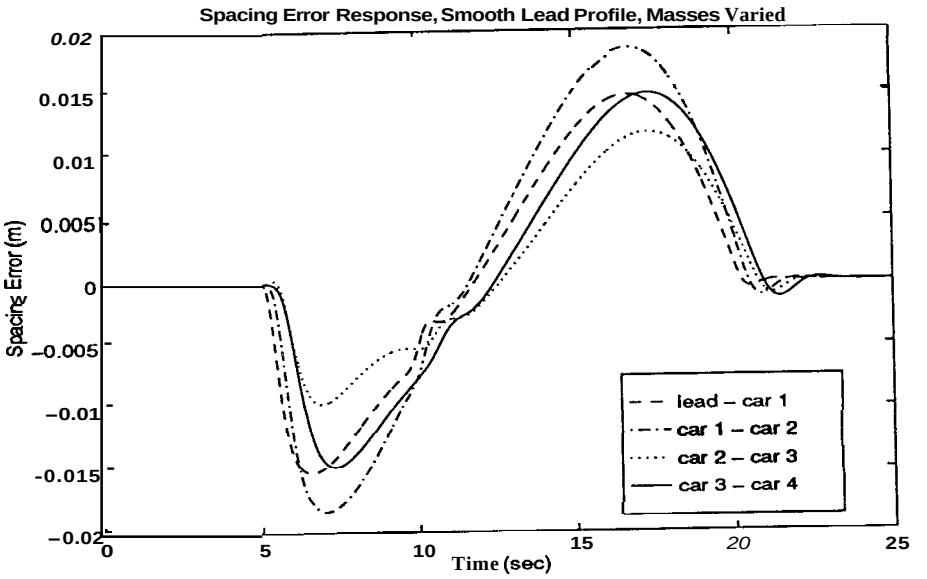

Figure 8: Spacing Error Responses of 4-car Platoons Following the "Smooth" Lead Profile for No Parametric Uncertainty and Uncertainty in Vehicle Masses (Car 2: 10%, Car 3 -10%)

a)

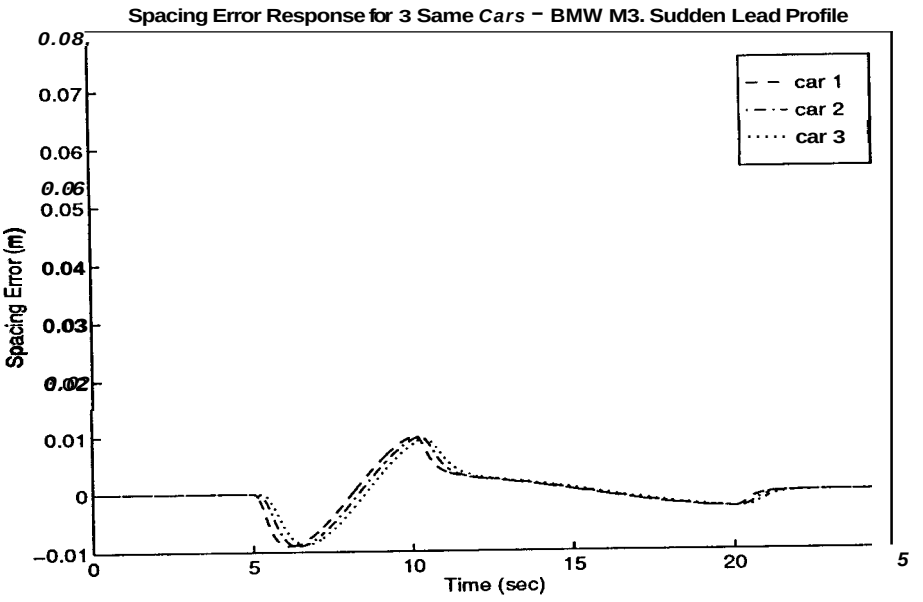

b)

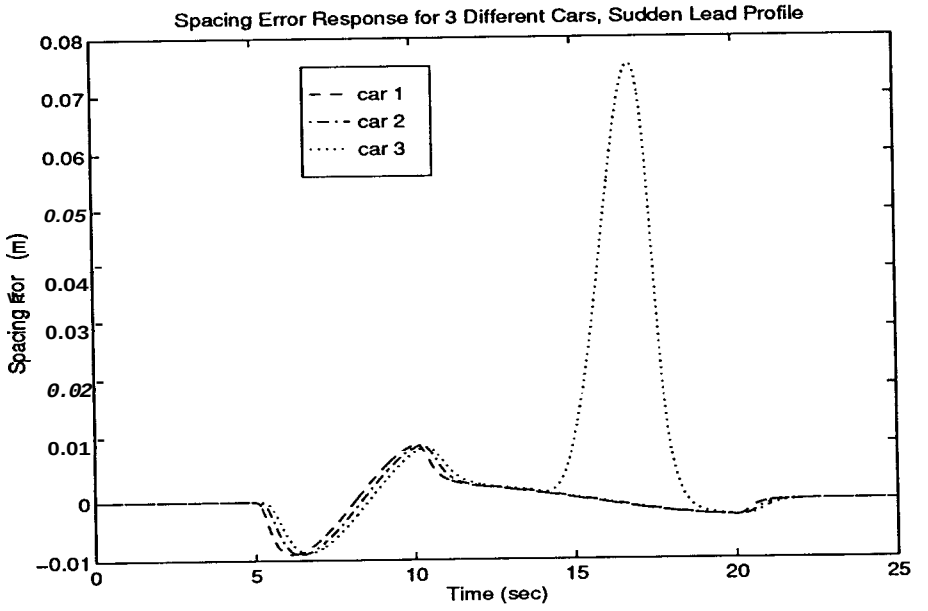

Figure 9: Spacing Error Responses of Platoons with Identical Cars and Different Cars Following Sudden Lead Profile

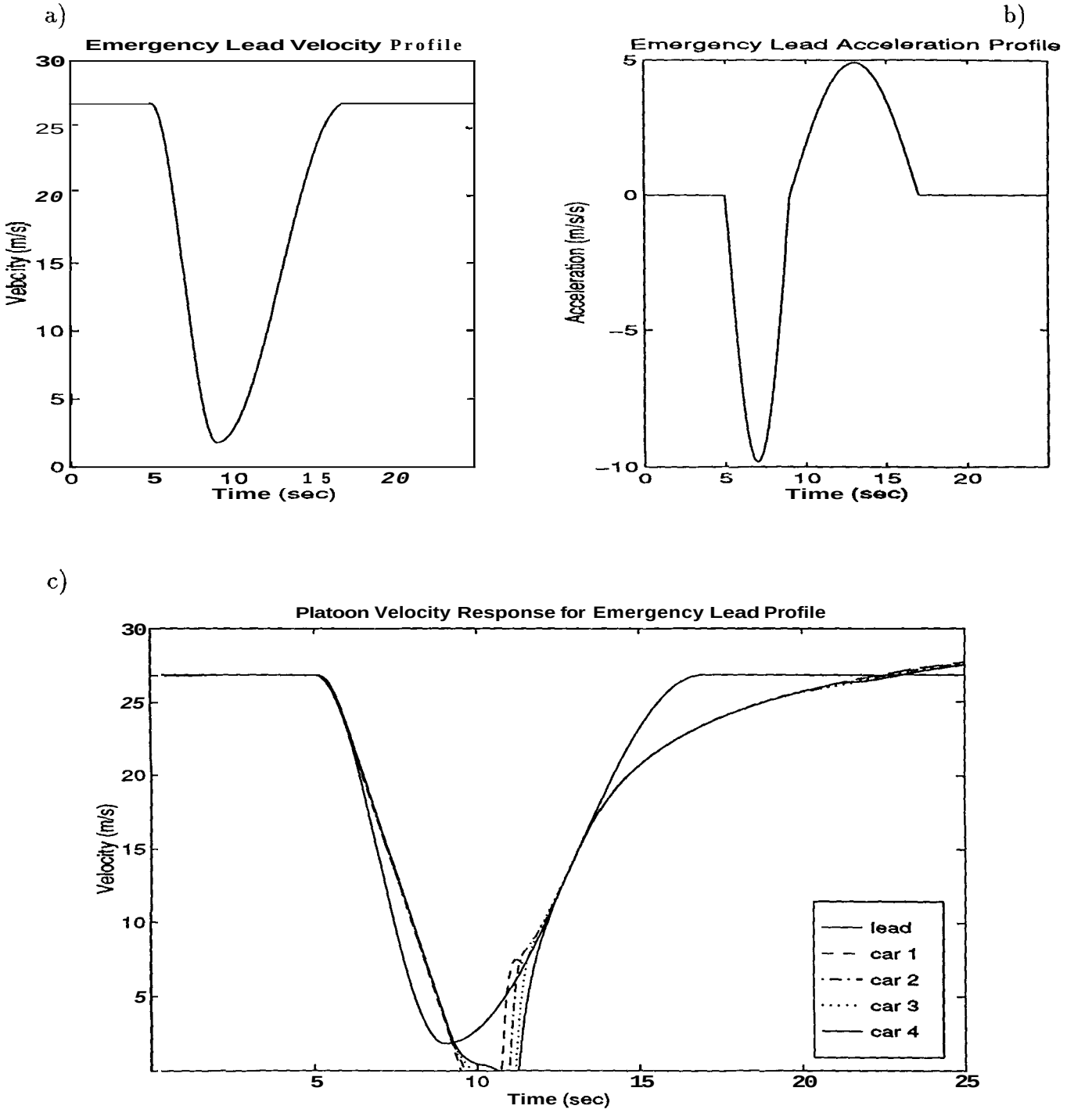

Figure 10: Emergency Lead Profiles and Platoon Velocity Response for Emergency Situation

A Platoon Modeling Equations

A.1 Powertrain model

The equations for the reduced order engine dynamics [32] are:

$$F_{e,m}(\phi, v) = \alpha \cdot (1 - e^{-\beta \cdot \phi})^{\gamma} \tag{1}$$

$$\tau_e(\dot{\phi}) = 2.0905 \cdot \dot{\phi}^{-0.7033} \tag{2}$$

where

$$\begin{aligned} \alpha &= 1.0 \times 10^{3} \cdot (-0.0053 \cdot v + 2.7404) \\ \beta &= 1.0 \times 10^{-3} \cdot (0.0613 \cdot v + 101.9315) \\ \gamma &= 1.0 \times 10^{-3} \cdot (18.8640 \cdot v + 855.0600) \end{aligned}$$

Further work to implement the equations for simulation [33] has reduced the dynamics to a first-order lag, where $\tau_e = 0.2$ sec, and limiting the engine thrust by the following saturation function:

$$F_{e,m}(v) = \alpha \cdot (1 - e^{-\beta \cdot 75.0})^{\gamma} \cdot (-0.0910 \cdot v + 3.5424) \tag{3}$$

where

$$\begin{aligned} \alpha &= 1.0 \times 10^{3} \cdot (-0.01908 \cdot v + 2.7404) \\ \beta &= 1.0 \times 10^{-3} \cdot (0.22068 \cdot v + 101.9315) \\ \gamma &= 1.0 \times 10^{-3} \cdot (67.9104 \cdot v + 855.0600) \end{aligned}$$

Replacing the above saturation function with power curve relationships has shown good results for various cars. Multiplying the maximum torque from the power curves by the gear ratios and drivetrain efficiency and dividing by the wheel base produces the maximum engine force transmitted through the tires:

$$F_{e,m} = PC(v) \cdot e_{ff} \cdot GR/h \tag{4}$$

where

$$\begin{aligned} T_{e,m} &= PC(\omega) \qquad \text{(given by car manufacturers)} \\ w &= v \cdot GR/h \end{aligned}$$

Adding a term for uncertainty in engine effectiveness yields:

$$F_{e,m} = PC(v) \cdot e_{ff} \cdot GR/h \cdot (1 + e_{un}) \tag{5}$$

A.2 Brake model

The equations for the brake torque [15] are:

$$\tau_b \cdot \dot{T}_b + T_b = \alpha \cdot T_{b,m} \tag{6}$$

where the simplified equation for the maximum brake torque is given by:

$$T_{b,m} = \mu \cdot M \cdot g \cdot h \cdot TR \tag{7}$$

Including the parametric variations gives:

$$T_{b,m} = \mu \cdot (1 + \mu_{un}) \cdot M \cdot (1 + M_{un}) \cdot g \cdot h \cdot TR \tag{8}$$

A.3 Aerodynamic drag

The force due to aerodynamic drag is [30]:

$$F_a = \frac{\rho}{2} \cdot CR_D \cdot C_D \cdot A \cdot (v + v_w)^2 \cdot sgn(v + v_w) \tag{9}$$

Including terms in the above equation to account for parametric variations gives:

$$F_a = \frac{\rho}{2} \cdot CR_D \cdot C_D \cdot CR_a \cdot (1 + C_{D,un}) \cdot A \cdot (v + v_w)^2 \cdot sgn(v + v_w) \tag{10}$$

A.4 Rolling Resistance

The force due to rolling resistance is [32]:

$$F_r = M \cdot g \cdot f_r \cdot \cos(\theta) \tag{11}$$

The simplified relationship for the coefficient of rolling resistance is [32]:

$$\begin{aligned} f_r \;=\; & (4.864 \times 10^{-4} \cdot G_o - 1.03 \times 10^{-8}) \cdot v^3 \\ & + (-0.0952 \cdot G_o + 1.1425 \times 10^{-6}) \cdot v^2 \\ & + (7.0982 \cdot G_o - 3.1010 \times 10^{-5}) \cdot v + 0.01 \end{aligned} \tag{12}$$

where

$$4.050 \times 10^{-7} \text{ (good)} \leq G_o \leq 6.400 \times 10^{-6} \text{ (poor) for highways}$$

Rewriting the above equation in terms of tire hysteresis, axle height, and uncertainty in the coefficient of rolling resistance (which includes changes in G_o), the relationship for the coefficient of rolling resistance becomes:

$$\begin{aligned} f_r \;=\; & \frac{a_h}{h} \cdot (-7.209 \times 10^{-14} \cdot v^3 + 7.877 \times 10^{-12} \cdot v^2 \\ & - 2.007 \times 10^{-10} \cdot v + 7.136 \times 10^{-8}) \cdot CF_r \cdot (1 + f_{r,un}) \end{aligned} \tag{13}$$

A.5 Gravitational force

The force due to road grade is [21, 32]:

$$F_g = M \cdot g \cdot \sin(\theta) \tag{14}$$

Including parametric variations in M gives:

$$F_g = M \cdot (1 + M_{un}) \cdot g \cdot \sin(\theta) \tag{15}$$

B Data Base

The following is a list of input profiles considered for platoon simulations.

B.1 Lead car acceleration profile

1. Nominal Operation — constant acceleration of 0 at all times
2. Smooth Deceleration/Acceleration — nominal operation with a half-sine deceleration magnitude of $0.1g$ for 5 sec followed by a half-sine acceleration magnitude of $0.05g$ for 10 sec
3. Sudden Deceleration/Acceleration — nominal operation with a half-sine deceleration magnitude of $0.2g$ for 5 sec followed by a half-sine acceleration magnitude of $0.1g$ for 10 sec
4. Emergency Deceleration/Acceleration — nominal operation with a half-sine deceleration magnitude of 1g for 4 sec followed by a half-sine acceleration magnitude of $0.5g$ for 8 sec

B.2 Wind velocity profiles

1. Nominal - constant wind velocity of 0
2. Fore Wind - constant wind of velocity 20 m/s
3. Aft Wind - constant wind of velocity -20 m/s
4. Sinusoidal Wind - sinusoidal wind of velocity magnitude 10 m/s and frequency 0.1 Hz

B.3 Road grade profiles

1. Nominal - constant grade of 0 rad
2. Uphill - constant grade of 0.06 rad
3. Downhill - constant grade of -0.06 rad
4. Sinusoidal Hills - sinusoidal grade of magnitude 0.03 rad and frequency 0.1 Hz

B.4 Road traction profiles

1. Nominal - constant traction of 1.00
2. Light Rain - constant traction of 0.75
3. Heavy Rain - constant traction of 0.52

C Vehicle Ride Quality

The vehicle ride quality measure developed by Leatherwood et al [10, 11] is employed for determining platoon ride comfort for longitudinal acceleration profiles. The steps for determining ride comfort are:

1. Compute power spectral density of longitudinal acceleration profile
2. Weight power spectral density using the weightings in Figure 5
3. Calculate weighted root mean square acceleration a_{wrms} from weight power spectral density
4. Determine discomfort number: $DISC = -0.02 + 42.24 \cdot a_{wrms}$

D Simulation Specifications

The following is a list of variables and other specifications used in platoon simulations and the worst case performance algorithm.

D.1 Parameters

These values were chosen for a typical mid-sized passenger vehicle employing the V6 engine model described by Equation 4:

$$\begin{aligned} A &= 1.75 m^2 & a_h &= 49{,}050 \text{ N m} \\ C_D &= 0.40 & g &= 9.81\ m/s^2 \\ h &= 0.35\, m & M &= 1800\, kg \\ \mu &= 0.78 & \rho &= 1.23\, kg/m^3 \\ \tau_b &= 0.2\ sec & \tau_e &= 0.2\ sec \end{aligned}$$

D.2 Parametric Uncertainties

The following are the weighting bounds chosen for the parametric uncertainties as described in Section 3.1:

$$\begin{aligned} e_{un} &= \pm 15\% \\ \mu_{un} &= \pm 25\% \\ M_{un} &= \pm 12\% \\ C_{D,un} &= \pm 15\% \\ f_{r,un} &= \pm 16\% \end{aligned}$$

with the weighting correction factors:

$$\begin{aligned} \text{CR,} &= 1.175 \\ CR_r &= 1.100 \end{aligned}$$

D.3 Input Specifications

The bounds chosen for the inputs are (Section 3.2):

$$\begin{aligned} -\log \leq\ & l_a & \leq\ & 7g \\ -20\ m/s \leq\ & \text{v,} & \leq\ & 20 m/s \\ -0.06\, rad \leq\ & 8 & \leq\ & 0.06\ \textit{rad} \\ 0.52 \leq\ & \text{TR} & \leq\ & 1.01 \\ -0.05 \leq\ & \text{SNR} & \leq\ & 0.05 \end{aligned}$$

where, during one simulation, v, will not vary more than $\pm$ 10 m/s and 8 not more than $\pm$ 0.03 rad.

D.4 Other Specifications

For other vehicles and engine types, the following information is used.

D.4.1 Gear shifting

The gear shifting mechanism with be illustrated by the following example. Let the gear ratios be:

$$GR_1 = 10.2,\ GR_2 = 7.4,\ \text{GR3} = 5.6,\ \text{GR4} = 3.8$$

where the subscript denotes the gear number. Also, let the gear shifting engine speeds (RPM) be:

$$\omega_{down} = 1500,\ \omega_{1\to 2} = 6300,\ \omega_{2\to 3} = 6200,\ \omega_{3\to 4} = 6100$$

where the subscript *down* denotes the engine speed for all gears at which down-shifting occurs and the subscripts $i \to i+1$ denote the engine speed at which gear i shifts up to gear $i+1$. Assume the vehicle was operating in gear 3, GR = 5.6. If $w \geq 6100 RPM$, then GR becomes 3.8 and the gear number changes to 4. If instead $w \leq 1500 RPM$, then GR becomes 7.4 and the gear number changes to 2. The engine speed is not allowed to fall below ω_{min} in 1st gear or go above ω_{max} in the highest gear.

D.4.2 1995 BMW M3

The power curve for a BMW sohc inline-4 engine has been curve-fitted to a seventh-order polynomial fit:

$$\begin{aligned} T_{e,m} = PC(\omega) = & -1.067 \times 10^{-22} \cdot \omega^7 + 2.7799 \times 10^{-18} \cdot \omega^6 - 2.944 \times 10^{-14} \cdot \omega^5 \\ & +1.6262 \times 10^{-10} \cdot \omega^4 - 5.0158 \times 10^{-7} \cdot \omega^3 + 8.5892 \times 10^{-4} \cdot \omega^2 \\ & -0.74307 \cdot \omega + 427.94 \end{aligned} \tag{16}$$

The final drive gear ratios are:

$$GR_1 = 13.230,\ GR_2 = 7.8435,\ GR_3 = 5.2290,\ GR_4 = 3.9060,\ GR_5 = 3.1500$$

The engine speeds at which shifting gears occur are approximately:

$$\omega_{down} = 1500,\ \omega_{1\to 2} = 6800,\ \omega_{2\to 3} = 6800,\ \omega_{3\to 4} = 6500,\ \omega_{4\to 5} = 6500$$

and

$$\omega_{min} = 1000,\ \omega_{max} = 6200$$

The following parameters which differ from the specifications in Section D.1 are:

$$\begin{aligned} A &= 1.877 m^2 & h &= 0.335\ m \\ M &= 1530\ kg & \mu &= 1.036 \end{aligned}$$

D.4.3 1995 Chevrolet Cavalier

The power curve for a GM 2.2L L4 engine employed in a Chevrolet Cavalier has been curve-fitted to a fifth-order polynomial fit:

$$\begin{aligned} PC(\omega) &= 4.653 \times 10^{-16} \cdot \omega^5 - 7.0184 \times 10^{-12} \cdot \omega^4 + 3.7748 \times 10^{-8} \cdot \omega^3 \\ &\quad -9.3837 \times 10^{-5} \cdot \omega^2 + 0.12466 \cdot w + 37.592 \end{aligned} \tag{17}$$

The final drive gear ratios are:

$$GR_1 = 13.998, \quad GR2 = 7.6970, \quad GR3 = 5.1910, \quad GR4 = 3.6874, \quad GR5 = 2.6492$$

The engine speeds at which shifting gears occur are approximately:

$$\omega_{down} = 1500, \quad \omega_{1\to2} = 6000, \quad \omega_{2\to3} = 6000, \quad \omega_{3\to4} = 6000, \quad \omega_{4\to5} = 5800$$

and

$$\omega_{min} = 1000, \quad \omega_{max} = 4150$$

The following parameters which differ from above are:

$$\begin{aligned} A &= 2.313\, m^2 & h &= 0.3348\, m \\ M &= 1330\, kg & \mu &= 0.783 \end{aligned}$$

D.4.4 1995 Monte Carlo 234

The power curve for a GM 3.4L V6 (LQ1) engine has been curve-fitted to a fifth-order polynomial fit:

$$\begin{aligned} PC(\omega) &= 1.5232 \times 10^{-16} \cdot \omega^5 - 2.9684 \times 10^{-12} \cdot \omega^4 + 2.1699 \times 10^{-8} \cdot \omega^3 \\ &\quad -8.1421 \times 10^{-5} \cdot \omega^2 + 0.17657 \cdot w + 27.964 \end{aligned} \tag{18}$$

The final drive gear ratios are:

$$GR_1 = 10.02, \quad GR_2 = 5.385, \quad GR_3 = 3.430, \quad GR_4 = 2.400$$

The engine speeds at which shifting gears occur are approximately:

$$\omega_{down} = 1500, \quad \omega_{1\to2} = 7000, \quad \omega_{2\to3} = 7000, \quad \omega_{3\to4} = 5400$$

and

$$\omega_{min} = 1500, \quad \omega_{max} = 3750$$

The following parameters which differ from above are:

$$\begin{aligned} A &= 2.100\, m^2 & h &= 0.3569\, m \\ M &= 1670\, kg & \mu &= 0.866 \end{aligned}$$

D.4.5 1995 GM 5.7L V8 (LTI) engine

The power curve for the GM 5.7L V8 (LT1) engine has been curve-fitted to a fifth-order polynomial fit:

$$\begin{aligned} PC(\omega) = \; & 4.9668 \times 10^{-16} \cdot \omega^5 - 9.9007 \times 10^{-12} \cdot \omega^4 + 7.1658 \times 10^{-8} \cdot \omega^3 \\ & -2.4759 \times 10^{-4} \cdot \omega^2 + 0.43510 \cdot w + 10.045 \end{aligned} \tag{19}$$

For a 1995 Chevrolet Impala SS for which this engine might be considered, the final drive gear ratios are:

$$GR_1 = 9.425, \;\; GR_2 = 5.020, \;\; GR3 = 3.080, \;\; GR_4 = 2.156$$

The engine speeds at which shifting gears occur are approximately:

$$\omega_{down} = 1000, \;\; \omega_{1\to 2} = 5500, \;\; \omega_{2\to 3} = 5500, \;\; \omega_{3\to 4} = 5500$$

and

$$\omega_{min} = 1000, \;\; \omega_{max} = 5500$$

References

[1] *Car & Driver,* "Long-Term Tests", Hachette Filipacchi Magazines, Inc., New York, issues Oct. 1994 - Dec. 1995.

[2] Cho, D. and Hedrick, J. K., *Automotive Powertrain Modeling for Control,* Transactions ASME Journal of Dynamic Systems, Measurement, and Control, Vol. III, No. 4, December 1989.

[3] Ebert, Nancy E., *SAE Tire Braking Traction Survey: A comparison of Public Highways and Test Surfaces,* SAE Technical Paper Series 890638.

[4] *Evaluation of Human Exposure to Whole-Body Vibration - Part 1: General Requirements,* International Organization for Standardization, ISO 2631/1, 1985.

[5] Harden Jr., Richard W., *Testing of Truck Tire Traction for Load and Aging Effects,* SAE Technical Paper Series 881872.

[6] Hegmon, Rudolph R., *Tire-Pavement Interaction,* SAE Technical Paper Series 870241.

[7] Hiltner, Edward; Arehart, Chuck; and Radlinski, Richard, *Light Vehicle ABS Performance Evaluation,* US Department of Transportation Final Report, DOT HS 807 813, December 1991.

[8] Kemp, I., *Influence of Front Tyre Wear on Wet Braking Performance of Medium Trucks,* SAE Technical Paper Series 881873.

[9] Kohmura, Shingo; Nakamura, Hideyuki; Komura, Junsuke; and Tanake, Yutaka, *Estimation of Tire Treadwear on a Vehicle,* SAE Technical Paper Series 910168.

[10] Leatherwood, Jack D. and Barker, Linda M., *A User-Oriented Computerized Model for Estimating Vehicle Ride Quality,* NASA Technical Paper 2299, 1984.

[11] Leatherwood, Jack D.; Dempsey, Thomas K.; and Clevenson, Sherman A., *A Design Tool for Estimating Passenger Ride Discomfort With Complex Ride Environments,* Human Factors 22(3), 1980, pp. 291-312.

[12] Lee, Richard A. and Pradko, Fred, *Analytical Analysis of Human Vibration,* SAE Technical Paper Series 680091.

[13] Lu, X. P., "Effects of Road Roughness on Vehicular Rolling Resistance," *Measuring Road Roughness and Its Effects on User Cost and Comfort, ASTM STP 884,* T. D. Gillespie and Michael Sayers, Eds., American Society for Testing and Materials, Philadelphia, 1985, pp. 143-161.

[14] Mazor, Steve D. and Matthews, Ken B., *Vehicle Testing to SAE Acceleration and Braking Recommended Practices,* SAE Technical Paper Series 861116.

[15] McMahon, Donn H. and Hedrick, J. Karl, *Longitudinal Model Development for Automated Roadway Vehicles,* PATH Research Report UCB-ITS-PRR-89-5, University of California at Berkeley, October 1989.

[16] McMahon, D. H.; Hedrick, J. K.; and Shladover, S. E., *Vehicle Modeling and Control for Automated Highway Systems,* Proceedings of the 1990 American Control Conference, San Diego, CA, 1990.

[17] Meyer, Wolfgang E. and Henry, John J., *Tire-Pavement Traction, Demand and Availability,* SAE Technical Paper Series 840071.

[18] Moyer, Ralph A. and Sjogren, Roy G., *Test Facility Requirements for the Measurement and Evaluation of Coefficients of Friction at the Tire-Road Interface and Their Relation to Highway and Vehicle Safety,* Hodges Transportation Inc., Carson City, Nevada, September 1967.

[19] Ramshaw, R. and Williams, T., *The Rolling Resistance of Commercial Vehicle Tyres,* Transport and Road Research Laboratory, Crowthorne, Berkshire, 1981.

[20] Rizenbergs, Rolands L. and Ward, Hugh **A.,** *Skid Testing with an Automobile an Interim Report,* Kentucky Department of Highways, February 1966.

[21] Sheikholeslam, Shahab and Desoer, Charles A., *Longitudinal Control of a Platoon of Vehicles I: Linear Model,* PATH Research Report UCB-ITS-PRR-89-3, University of California at Berkeley, August 18, 1989.

[22] Sheikholeslam, Shahab and Desoer, Charles **A.,** *Longitudinal Control of a Platoon of Vehicles; 11: First and Second Order Time Derivatives of Distance Deviations,* PATH Research Report UCB-ITS-PRR-89-6, University of California at Berkeley, December 1989.

[23] Sheikholeslam, Shahab and Desoer, Charles **A.,** *Longitudinal Control of a Platoon of Vehicles; III: Nonlinear Model,* PATH Research Report UCB-ITS-PRR-90-1, University of California at Berkeley, April 1990.

[24] Sheikholeslam, Shahab and Desoer, Charles A., *Longitudinal Control of a Platoon of Vehicles,* ASME Journal of Dynamics, Control, and Measurement, submitted June 1990

[25] Sheikholeslam, Shahab and Desoer, Charles **A.,** *Longitudinal Control of a Platoon of Vehicles with no Communication of Lead Vehicle Information,* Proceedings of the American Control Conference, Vol. 3, 1991, pp. 3102-3106.

[26] Shladover, S. E., *Longitudinal Control of Automated Guideway Transit Vehicles Within Platoons*, ASME Journal of Dynamics, Control, and Measurement, vol. 100, December 1978, pp. 302-310.

[27] *SIMULINK User's Guide*, The Mathworks, Inc., Massachusetts, March 1992.

[28] Smith, C. G.; McGehee, D. Y.; and Healey, **A.** J., *The Prediction of Passenger Riding Comfort from Acceleration Data*, **ASME** Journal of Dynamic Systems, Measurement, and Control, vol. 100, March 1978, pp. 34-41.

[29] Swaroop, D. V. **A.** H. ***G.,*** *String Stability of Interconnected Systems: An Application to Platooning in Automated Highway Systems*, Ph.D. Thesis, Vehicle and Dynamics Laboratory, University of California at Berkeley, 1994

[30] Tongue, Benson H.; Moon, Ahrie; and Harriman, Douglas, *Low Speed Collision Dynamics: Second Year Report*, PATH Research Report, University of California at Berkeley, submitted December 1995.

[31] Tongue, Benson H.; Packard, Andy; and Sachi, Paul, *Qualitative Analysis on the Performance of Non-uniform Platoons: Report 11, Worst Case Platoon Performance*, PATH Research Report, University of California at Berkeley, submitted May 1996.

[32] Tongue, Benson H.; Yang, Yean-Tzong; and White, Matthew T., *Platoon Collision Dynamics and Emergency Maneuvering I: Reduced Order Modeling of a Platoon for Dynamical Analysis*, PATH Research Report UCB-ITS-PRR-91-15, University of California at Berkeley, August 1991.

[33] Tongue, Benson H. and Yang, Yean-Tzong, *Platoon Collision Dynamics and Emergency Maneuvering II: Platoon Simulations for Small Disturbances*, PATH Research Report UCB-ITS-PRR-94-4, University of California at Berkeley, February 1994.

[34] Tongue, Benson H. and Yang, Yean-Tzong, *Platoon Collision Dynamics and Emergency Maneuvering III: Platoon Collision Models and Simulations*, **PATH** Research Report UCB-ITS-PRR-94-02, University of California at Berkeley, February 1994.

[35] Tongue, Benson H. and Yang, Yean-Tzong, *Platoon Collision Dynamics and Emergency Maneuvering IV: Intra-Platoon Collision Behavior and a New Control Approach for Platoon Operation During Vehicle Exit/Entry - Final Report*, PATH Research Report UCB-ITS-PRR-94-25, University of California at Berkeley, November 1994.

[36] Yarmus, Joseph; Walter, Robert; and Mengert, Peter, *Statistical Analysis of Tire Treadwear Data*, U.S. Department of Transportation, Washington, DC, May 1985.